Low Reynolds Number Tests of NACA 64-210, NACA 0012, and Wortmann FX67-K170 Airfoils in Rain

R. John Hansman Jr.* and Anthony P. Craig†
Massachusetts Institute of Technology, Cambridge, Massachusetts

Wind-tunnel experiments were conducted on Wortmann FX67-K170, NACA 0012, and NACA 64-210 airfoils at a simulated rain rate of 1000 mm/h and Reynolds number of 3.1×10^5 to compare the aerodynamic performance degradation of the airfoils in heavy rain conditions and to identify the various mechanisms that affect airfoil performance in rain conditions. Lift and drag were measured in both dry and wet conditions, and a variety of flow-visualization techniques were employed. At low angles of attack, the lift degradation in wet conditions varied significantly between the airfoils. The Wortmann section had the greatest lift degradation (~25%) and the NACA 64-210 airfoil had the least (~5%). At high angles of attack, the NACA 64-210 and NACA 0012 airfoils were observed to have improved aerodynamic performance in rain conditions due to a reduction of boundary-layer separation. Performance degradation in heavy rain for all three airfoils at low angles of attack could be emulated by forced boundary-layer transition near the leading edge. Time-resolved measurements indicate two primary mechanisms are responsible for the observed performance degradation. The initial effect of rain is to cause premature boundary-layer transition at the leading edge. The second effect occurs at time scales consistent with top surface water runback (1–10 s). The runback layer is thought to alter the airfoil geometry effectively, but this effect is most likely exaggerated in these tests due to the small scale. The severity of the performance degradation for the airfoils varied. The relative differences appeared to be related to the susceptibility of each airfoil to premature boundary-layer transition.

Nomenclature

C_D	= drag coefficient
C_L	= lift coefficient
C_M	= moment coefficient
FT	= location of forced boundary-layer transition
L/D	= lift-to-drag ratio
R	= boundary-layer reattachment point
Re	= Reynolds number
S	= boundary-layer separation point
T	= boundary-layer transition point

Introduction

THE aerodynamic penalty associated with flight through heavy rain has recently been postulated to be a contributing cause in several severe weather accidents.[1] Performance degradation in rain and accompanying change in stall behavior could be a significant consideration in determining the optimum microburst escape procedure. Rain-induced aerodynamic effects also influence the pitch stability of canard aircraft configurations[2] and may significantly alter the performance of natural laminar flow aircraft.

In subscale wind-tunnel experiments, varied performance changes due to rain have been measured. Dunham et al.[3] observed reductions of up to 20% in the maximum lift coefficient for a transport-type airfoil in a multielement landing configuration under simulated heavy rain at Reynolds numbers of approximately 1.7×10^6. The loss of lift was accompanied by an increase in drag and a reduction of up to 8 deg in the stall angle of attack. However, for the same airfoil in a single-element cruise configuration, minimal performance degradation was measured in heavy rain conditions at low angles of attack and increases in aerodynamic performance at high angles of attack were observed. Dunham[4] also reports a 15% decrease in the maximum lift coefficient for both flapped and unflapped NACA 0012 airfoils in heavy rain. In lower Reynolds number tests ($\sim 3 \times 10^5$), Hansman and Barsotti[5] and Marchman et al.[6] observed significant performance losses for natural laminar flow airfoils in heavy rain with maximum L/D losses as high as 75%.

In order to attempt to understand the mechanisms that cause the varied performance penalties observed in rain conditions, a series of controlled experiments was conducted at subscale for three airfoil types. The small scale of the experiments allowed comparative testing and detailed investigation of the physical mechanisms through which rain affects aerodynamic performance. The results can be directly applied to low Reynolds number applications, such as individual components of multielement airfoils, mini-remotely piloted vehicles (RPVs), and sailplanes. However, care must be used when extrapolating the results to full-scale cases due to complex scaling considerations. The test results do, however, provide insight into heavy rain degradation mechanisms and can provide a basis for higher Reynolds number investigations.

Summary of Approach

Wind-tunnel experiments were conducted on three airfoils to determine and compare the quantitative and qualitative effects of heavy rain on aerodynamic performance. A Wortmann FX67-K170, an NACA 0012, and an NACA 64-210 airfoil were tested. Lift and drag forces were measured for each of the airfoils in dry and wet (rain) conditions. The primary mechanism of the aerodynamic performance degradation in heavy rain is thought to be a premature boundary-layer transition due to the presence of the highly irregular water layer.[1,5,7] In order to assess the extent to which the observed performance degradation under wet conditions may have been due to premature boundary-layer transition, force measurements were made on the airfoils with the boundary layer intentionally tripped at various positions.

Received Nov. 20, 1986; presented as Paper 87-0259 at the AIAA 25th Aerospace Sciences Meeting, Reno, NV, Jan. 12–15, 1987, revision received Feb. 3, 1987.

*Assistant Professor, Aeronautics and Astronautics. Member AIAA.
†Research Assistant, Aeronautics and Astronautics. Student Member AIAA.

Time-dependent effects were investigated at low and high angles of attack by recording the change in lift of each airfoil when rain was initiated. The lift output was compared to time-resolved video photographs taken of the water behavior on the top surface of the airfoils in an attempt to correlate lift changes with water behavior.

Techniques were developed to study separation and boundary-layer transition under dry and wet conditions. The separation behavior of the NACA 64-210 airfoil was examined on the top surface of the airfoil by microtufts protected from water by a controlled water runback technique. The initial laminar to turbulent transition behavior in rain was investigated for the Wortmann FX67-K170 airfoil using liquid crystal boundary-layer visualization techniques.[8]

A computational fluid dynamics (CFD) code that predicts airfoil boundary-layer behavior[9,10] was employed to gain insight into the effect of rain on airfoil aerodynamics. The CFD code was used to illustrate the effect of premature boundary-layer transition on airfoil performance.

Experimental Technique

Airfoils Tested

The three airfoils chosen for the comparison are shown in Fig. 1. They are 1) a Wortmann FX67-K170 airfoil, 2) an NACA 0012 airfoil, and 3) an NACA 64-210 airfoil. These sections were chosen because each exhibits slightly different aerodynamic behavior. The Wortmann airfoil is a naturally laminar flow airfoil typically used on sailplanes. It has been found, in high-performance sailplanes, to be operationally susceptible to heavy rain. The NACA 64-210 airfoil is designed to operate with a turbulent boundary layer and is similar to those used on transport-category aircraft in cruise configuration. The NACA 0012 airfoil was chosen because it is a simple, symmetric airfoil and was expected to have intermediate boundary-layer behavior. In addition, all three airfoils were tested previously in heavy rain conditions, and the NACA 64-210 and NACA 0012 airfoils were part of a joint effort with NASA Langley Research Center to investigate scaling behavior of rain effects.

Lift and Drag Measurements

Figure 2 is a schematic view of the wind-tunnel setup used for the experiments. Each airfoil tested had a 6 in. chord (15.24 cm) and a 1 ft span (30.48 cm) and was held in the 1×1 ft MIT low-turbulence wind tunnel by a 2-axis external force balance, which measured lift and drag. Because of the comparative nature of these tests, no corrections were made due to wind-tunnel blockage effects. The airfoil's angle of attack was referenced to the airfoil's mean geometric chord line. Water droplets were introduced 1.5 m upstream of the airfoil by three rain simulation nozzles placed on the top and sides of the wind tunnel. The nozzles pointed downstream and were positioned to generate an even distribution of droplets in the test area. The droplet diameters produced by these nozzles varied within the range 0.1–0.9 mm. The amount of water in the wind tunnel, or liquid water content (LWC), could be controlled by varying the internal pressure of the water tank supplying the nozzles. A liquid water content of 30 g/m^3 was used as a test case. This corresponds to an extremely high rain rate of 1000 mm/h. The freestream tunnel velocity was measured upstream of the nozzles by a conventional pitot tube, micromanometer system. A freestream velocity of 70 mph was normally used for the wind-tunnel tests corresponding to a chord Reynolds number of 31×10^5.

In order to record time-dependent lift and drag force data, a chart recorder was employed. Because the force balance system had a natural oscillation frequency of approximately 11 Hz, the output was low-pass filtered at 10 Hz. To help analyze the time-dependent output, a strobe-synchronized video camera provided stop-action photographs of the water runback behavior on the top surface of the airfoils with 0.03-s time resolution. This technique provided a valuable tool for correlating the unsteady force output with the actual water behavior on the airfoil.

Flow Visualization

Various flow-visualization techniques were used to help determine the behavior on the top surface of the airfoils in dry and wet conditions. In order to visualize boundary-layer separation, microtufts were positioned on the top surface of the NACA 64-210 airfoil. However, because the tufts indicate separation incorrectly when wet, a technique was developed to protect the tufts in rain conditions (see Fig. 3). The runback pattern around the tufts was controlled by placing wax on the surface of the airfoil in a wedge pattern. Because of the relatively high surface forces achieved at the wax interface, the water runback avoided the waxed portion of the airfoil and kept the tufts dry. This method showed clear differences in separation behavior between dry and wet conditions for high-angle-of-attack cases.

In order to visualize boundary-layer transition, liquid crystals[8] were applied to the top surface of the airfoils. The liquid crystals indicate variations in shear stress by color change. Laminar to turbulent transition is, therefore, seen as a color discontinuity. The presence of water over the liquid crystals prevented accurate observation of the color changes. High-speed video photography was used to record the movement of the transition front prior to the development of water runback.

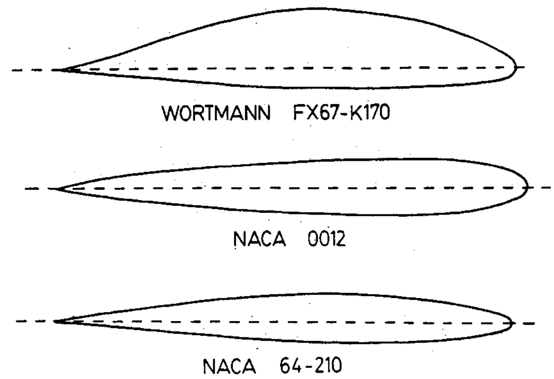

Fig. 1 Airfoil sections tested in rain conditions.

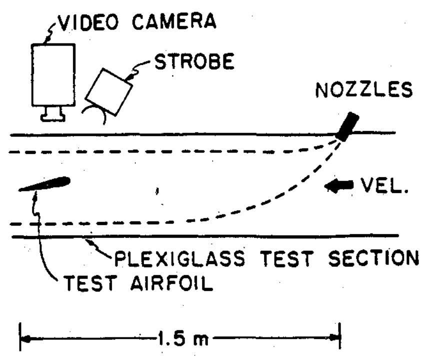

Fig. 2 Schematic view of wind tunnel setup.

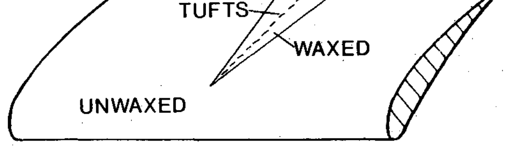

Fig. 3 Schematic view of tuft protection technique.

Experimental Results

Lift and Drag Force Data

Figures 4, 5, and 6 present lift and drag polar data for the Wortmann FX67-K170, NACA 0012, and NACA 64-210 airfoils, respectively, in dry and wet conditions. The tests were conducted at a Reynolds number of 3.1×10^5 and equivalent rain rate of 1000 mm/h. All three airfoils show a decrease in lift and an increase in drag due to heavy rain at low angles of attack. However, the magnitude of the degradation varies for the three airfoils. The Wortmann airfoil shows the greatest performance degradation. The overall lift coefficient is reduced by approximately 25% in heavy rain due to a reduction in slope and a downward shift of the lift polar. The maximum L/D is reduced by 50%. The NACA 0012 airfoil also has a reduction in the slope of the lift curve in wet conditions that corresponds to a reduction in lift of approximately 15% at low angles of attack. The NACA 64-210 airfoil has minimal lift degradation in heavy rain conditions. All three airfoils have a 20% overall increase in drag. However, the drag increase may be partially attributed to the high droplet momentum transfer induced by the heavy test rain rate.

At high angles of attack, above stall initiation, the effect of rain varies. Both the NACA 0012 and NACA 64-210 airfoils have an unexpected performance enhancement. The stall angle for the NACA 0012 airfoil is shifted from 14 deg in dry conditions to 18 deg in wet conditions. For the NACA 64-210 airfoil, stall initiation occurs at approximately the same angle of attack in both dry and wet conditions (12 deg). However, the lift performance of the NACA 64-210 at high angles of attack increases in wet conditions compared to dry conditions. At high angles of attack, the lift polar for the Wortmann airfoil in dry conditions is erratic, indicating the presence of a complicated stall process, which is thought to be related to the low Reynolds number boundary-layer behavior. In wet conditions, the lift polar of the Wortmann is much smoother, but has an accompanying decrease in performance compared to the dry conditions.

Forced Boundary-Layer Transition Results

Previous wind-tunnel experiments performed by Hansmann and Barsotti[5] suggest that premature boundary-layer transition causes the aerodynamic performance losses measured for natural laminar airfoils at low Reynolds numbers in heavy rain conditions. To investigate this hypothesis, boundary-layer transition elements were placed on the suction and pressure surfaces of each airfoil. Trip strips 0.25 in. wide and made up of sand grains ranging in diameter from 0.025 to 0.040 in. were placed at the 5, 25, 50, or 75% chordwise station on the top and bottom surface of each airfoil. Trip strips on the lower surface of the airfoils resulted in minimal performance changes, whereas forcing boundary-layer transition on the upper surface resulted in fairly significant performance changes. Therefore, the location of the lower trip strip was generally fixed at 5% chord, and the upper trip strip location was varied.

The results of the forced boundary-layer transition tests are shown in Figs. 7–9. For each airfoil, the trip strip position that best models the wet behavior is shown. This does not necessarily imply that transition occurs at these specific locations in wet conditions. It merely indicates the ability to model the wet behavior with trip strips at some location on the airfoil.

For the NACA 0012 and 64-210 airfoils, trip strips at 5% chord on the top surface best modeled the wet conditions. The behavior of the Wortmann airfoil in wet conditions was best emulated with trip strips placed at 25% chord on the top surface. When transition was forced at 5% chord on the upper

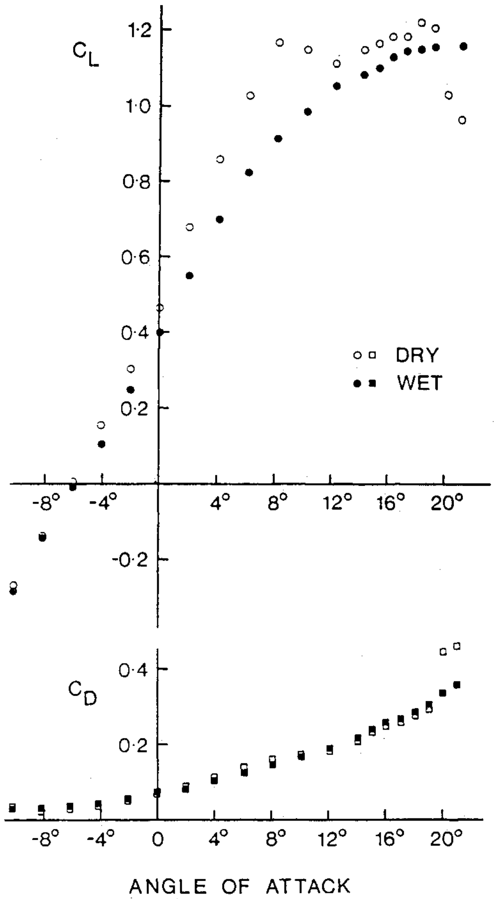

Fig. 4 Lift and drag coefficient vs angle of attack for the Wortmann FX67-K170 airfoil in dry and wet conditions.

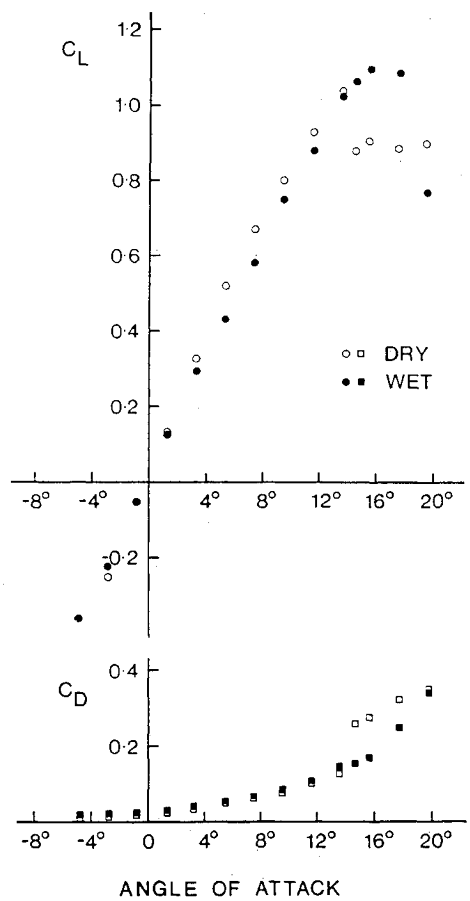

Fig. 5 Lift and drag coefficient vs angle of attack for the NACA 0012 airfoil in dry and wet conditions.

surface of the Wortmann airfoil, the performance measured became considerably worse than the observed performance of the airfoil in wet conditions. The favorable pressure gradient, which extends to approximately 40% chord for the Wortmann airfoil, may act to decrease the instability growth rate in the boundary layer. This would delay transition even in wet conditions on this airfoil and explain the successful wet performance emulation by roughness elements at 25% chord. However, the aft position of the transition emulation point may also be an indication that the sand grain size used in these tests is too large to emulate the water roughness, and so excessive degradation is observed when the grains are placed at 5% chord.

In general, the magnitude of the low-angle-of-attack airfoil performance degradation in wet conditions is emulated well by placing trip strips near the leading edge of each of the airfoils. However, the high-angle-of-attack behavior of the NACA 0012 and 64-210 airfoils is not emulated by these elements, possibly because the trip strips are aft of the leading-edge separation point. The overall ability to model heavy rain performance degradation with trip strips suggests that the aerodynamic degradation is caused by premature boundary-layer transition at low angles of attack.

Low-Angle-of-Attack Behavior

In order to understand better the mechanisms resulting in performance degradation in heavy rain, time-dependent lift and drag force output was recorded at low angles of attack and correlated with video observations of the water runback behavior on the upper surface of the airfoils. Observations were limited to the upper surface because the lower surface generally became uniformly wet immediately upon rain initiation. In addition, the results from the forced transition experiments indicate that the upper surface is the more critical of

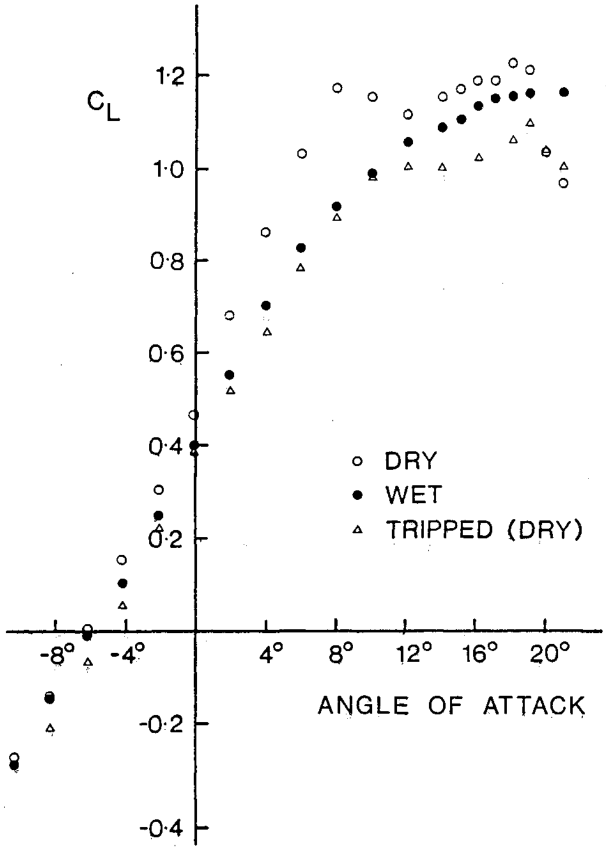

Fig. 7 Dry, wet, and artificially tripped (25% chord top, 5% chord bottom) lift polars for the Wortmann FX67-K170 airfoil.

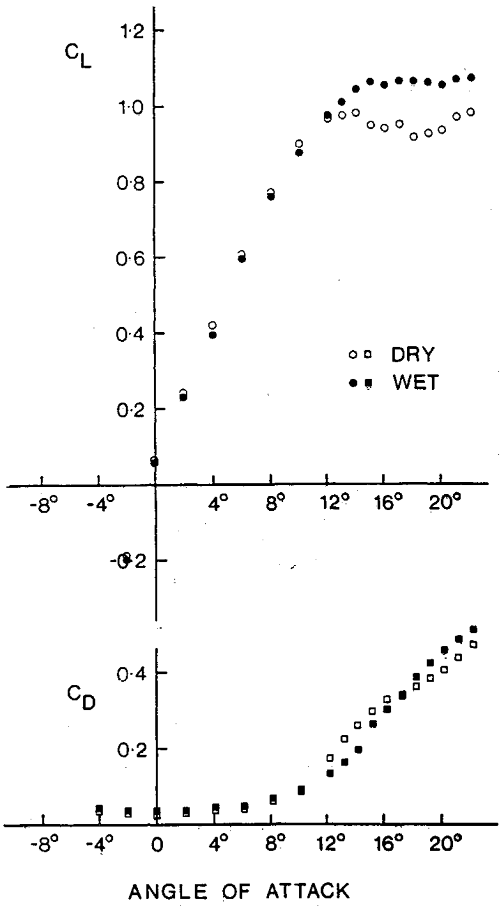

Fig. 6 Lift and drag coefficient vs angle of attack for the NACA 64-210 airfoil in dry and wet conditions.

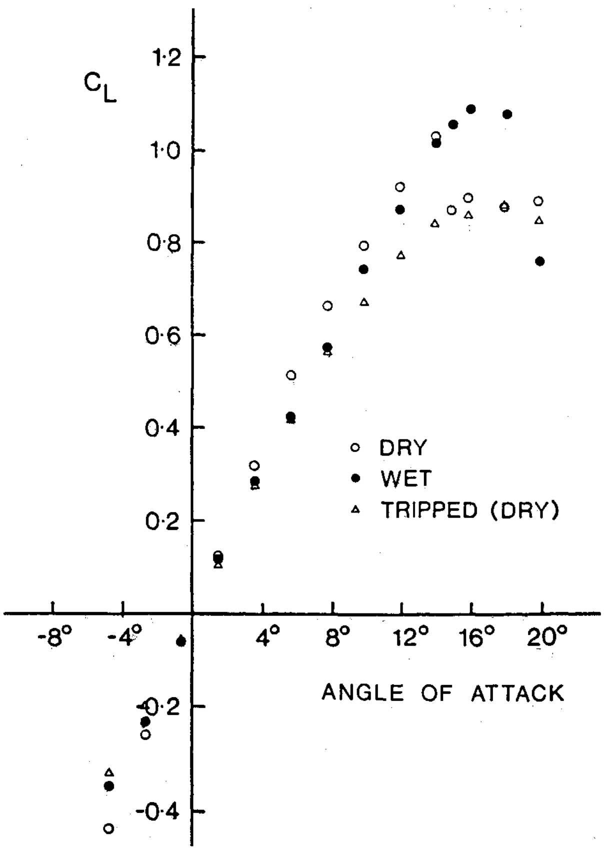

Fig. 8 Dry, wet, and artificially tripped (5% chord top) lift polars for the NACA 0012 airfoil.

the two surfaces. Because of the high droplet momentum transfer and the low signal-to-noise ratio in the drag output, only time-dependent lift output is presented and discussed.

Wortmann FX67-K170 Airfoil

Figure 10 shows the results for the Wortmann airfoil at 2-deg angle of attack. Both time-dependent lift output and water runback behavior are presented. The water runback graph indicates the average position of the runback front with respect to time after the water is turned on. Spanwise variations in the runback behavior are not shown. Typically however, spanwise variations in the runback front position are less than 15% chord. In some cases, water appears at the trailing edge and progresses forward. This can be seen in Fig. 10 at approximately 0.9 s. This phenomenon is an indication of a trailing-edge separation as the water is forced from the lower surface around the trailing edge to the upper surface.

Two distinct time-scale effects are present in the lift output. Initially, within the first 0.2 s, there is a significant loss of lift. This time scale is consistent with the response of the experimental force balance to a step input (0.1 s at 10 Hz) and is the same order of magnitude as the unsteady time scale found for an airfoil that encounters a sudden gust or undergoes a sudden change in angle of attack.[11] At this time, water on the airfoil surface is present only near the leading edge at less than 20% chord. This rapid loss of lift appears to be a result of premature transition of the boundary layer, which occurs near the leading edge. This hypothesis is confirmed by liquid crystal observations. In dry conditions, the liquid crystals indicate boundary-layer transition at the 65% chord station. Within 0.30 s after rain initiation, the boundary-layer transition point moves to within 20% of the leading edge, as indicated by the crystals with the video photography. Because the water layer extends to 20% chord, the exact location of the boundary-layer transition point is not known; however, it may be farther forward than 20% chord.

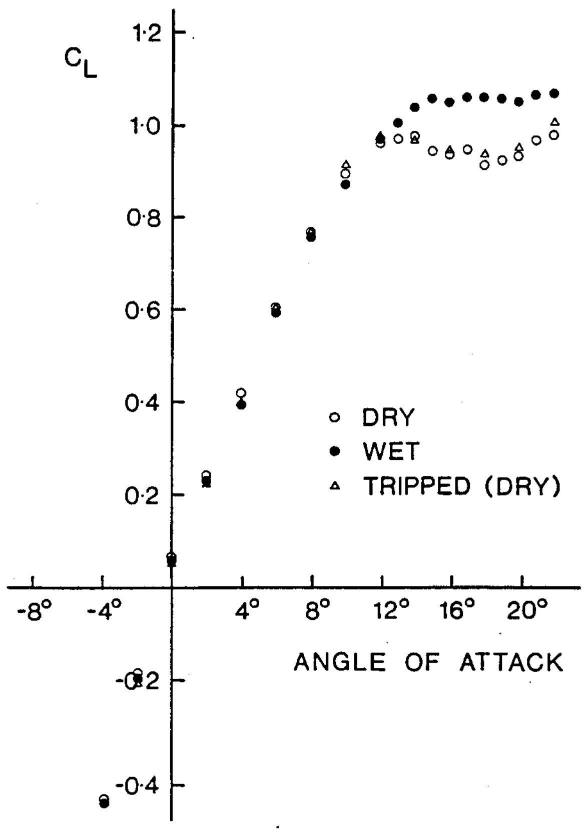

Fig. 9 Dry, wet, and artificially tripped (5% chord top) lift polars for the NACA 64-210 airfoil.

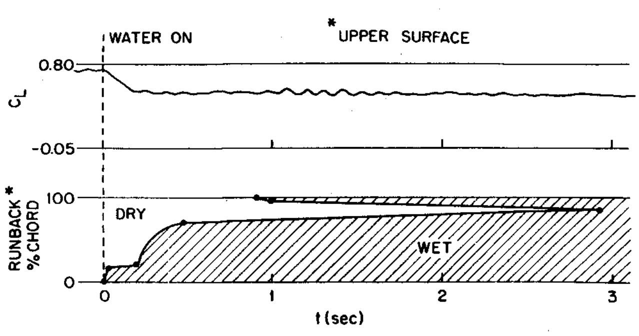

Fig. 10 Time-dependent lift and water runback position for the Wortmann FX67-K170 airfoil at 2-deg angle of attack.

The CFD code likewise predicts boundary-layer transition at 65% chord in dry conditions at a Reynolds number of 3.1×10^5. When boundary-layer transition is forced at the leading edge in the code, the resulting change in the lift coefficient is consistent with the differences noted in the dry and wet conditions in the experimental data. Figure 11 shows CFD results for the Wortmann airfoil at 2 deg when boundary-layer transition is allowed to occur naturally and when it is forced near the leading edge. Separation, transition, reattachment, and forced transition locations are indicated in the figure by the letters S, T, R, and FT, respectively. For the unforced case, transition is caused by a relatively large laminar separation bubble. In wet conditions, transition is caused by the roughness of the water surface. For these low Reynolds number tests, a laminar separation bubble is the predominant transition mechanism for all three airfoils in dry conditions, while roughness induces transition in wet conditions.

Another phenomenon apparent in the water behavior at low angles of attack is a trailing-edge separation present in the rain conditions. At about 0.9 s, water is drawn from the lower surface to the upper surface at the trailing edge of the airfoil, as indicated in Fig. 10. As observed in the video photography, the water layer in the region from 80% chord to the trailing edge moves very slowly and thickens considerably compared to the water layer forward of the 80% chord location. This indicates that a boundary-layer separation exists at approximately 80% chord. The CFD code also predicts a trailing-edge separation at approximately 80% chord when transition is forced at the leading edge. The separation can be seen for the forced CFD case in Fig. 11. In dry conditions, the trailing-edge separation is not predicted by the code (Fig. 11) and is not observed in tuft studies of the airfoil. These results are consistent with other studies that indicate that a trailing-edge separation is not uncommon when an airfoil's boundary layer is transitioned prematurely.

After the initial lift loss, an additional performance change occurs at a time scale consistent with the full-chord water runback time (Fig. 10). After that time, no further gross changes in the lift are seen. This behavior is observed for each of the airfoils at low angles of attack where there is a lift change associated with the runback time scale. The water layer is thought to cause an effective change in the airfoil geometry. It should be noted, however, that because of the small scale of the models employed in these experiments, the ratio of the water layer thickness to the chord length is artifically high. Therefore, the significance of the water layer geometry effects is likely enhanced in these small-scale tests.

NACA 0012 Airfoil

Figure 12 shows the time-dependent output for the NACA 0012 airfoil at 2-deg angle of attack. The magnitude of the lift degradation is less than for the Wortmann airfoil at 2 deg angle of attack, but the mechanisms appear to be the same. There is an immediate loss of lift initially, related to the boundary-layer transition mechanisms as well as a slower, secondary degradation correlated with the water runback. For

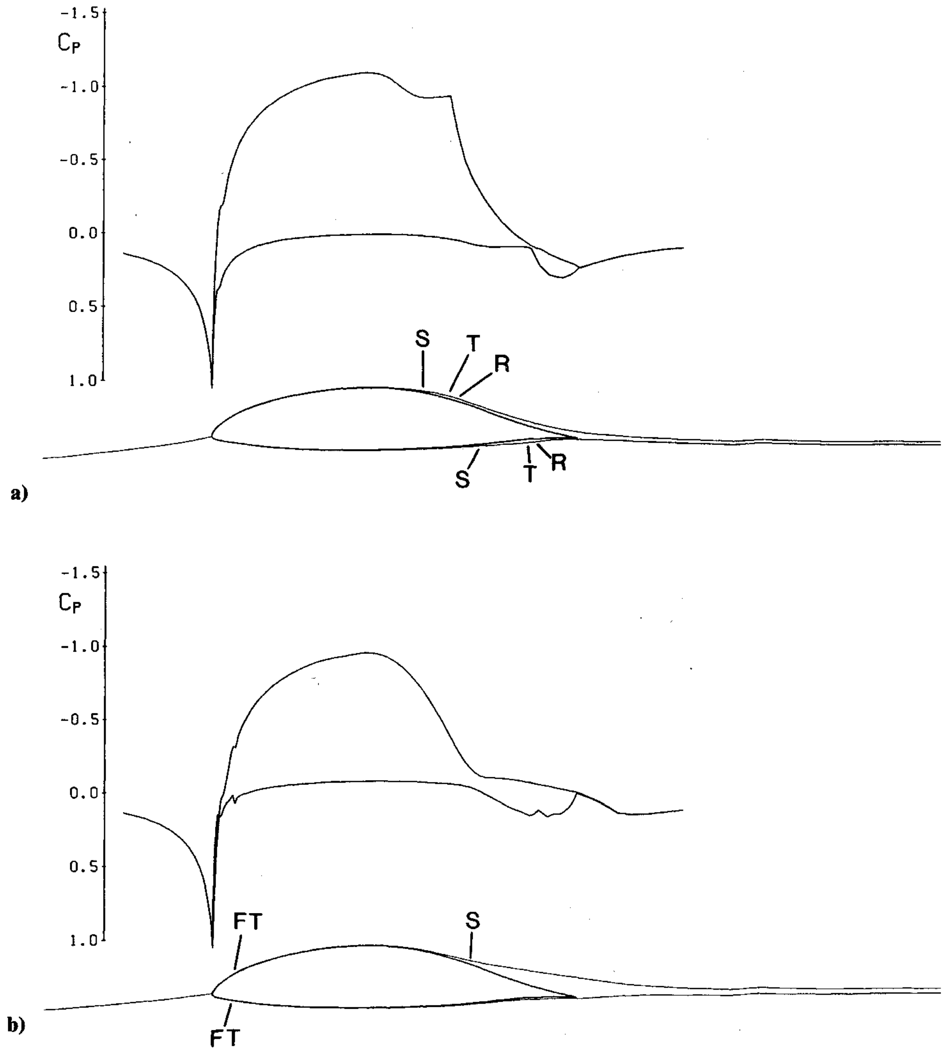

Fig. 11 Computer-generated flowfield and pressure distribution for the Wortman FX67-K170 airfoil at 2-deg angle of attack for a) natural transition and b) forced transition at 5% chord on the top and bottom surfaces. Boundary-layer separation (S), transition (T), reattachment (R), and forced transition (FT) locations are indicated.

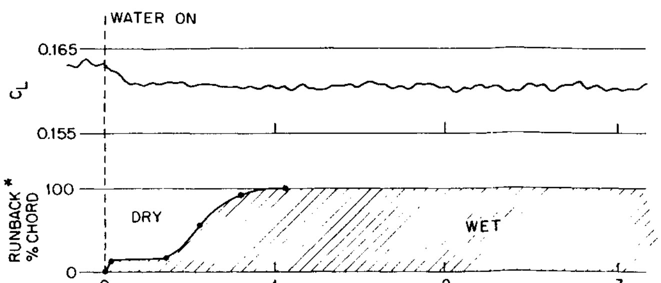

Fig. 12 Time-dependent lift and water runback position for the NACA 0012 airfoil at 2-deg angle of attack.

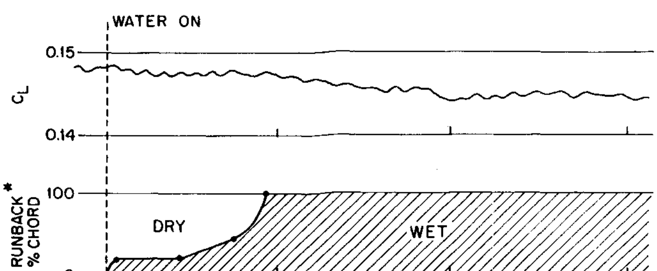

Fig. 13 Time-depdendent lift and water runback position for the NACA 64-210 airfoil at 1-deg angle of attack.

the dry case, the CFD code predicts boundary-layer transition at about 55% chord, indicating a fairly significant laminar flow portion. When transition is forced at the leading edge in the CFD code, the performance degradation is again consistent in magnitude with the experimental results. No trailing-edge separation resulting from premature boundary-layer transition is indicated for this airfoil at 2-deg angle of attack by either experimental or computational methods.

NACA 64-210 Airfoil

The time-dependent output for the NACA 64-210 airfoil at 1-deg angle of attack is shown in Fig. 13. The time-dependent lift behavior differs from the NACA 0012 or Wortmann airfoils in that the initial lift degradation is small compared to the degradation at longer runback time scales. The magnitude of the total change in lift coefficient for the NACA 0012 airfoil (Fig. 12) and the NACA 64-210 airfoil (Fig. 13) is nearly

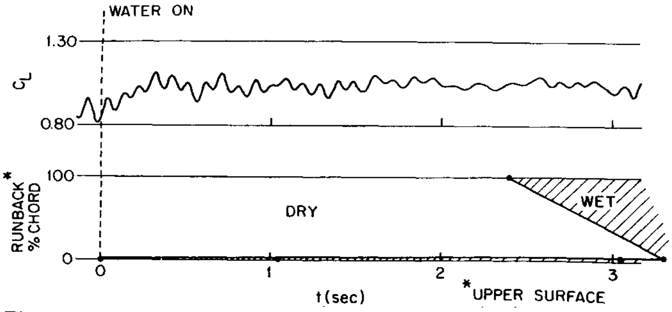

Fig. 14 Time-dependent lift and water runback position for the NACA 64-210 airfoil at 15-deg angle of attack.

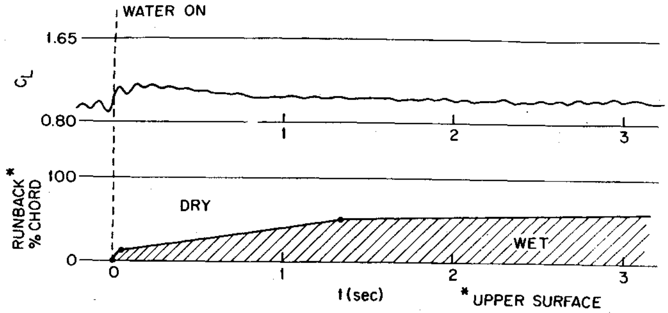

Fig. 16 Time-dependent lift output and water runback position for the NACA 0012 airfoil at 15-deg angle of attack.

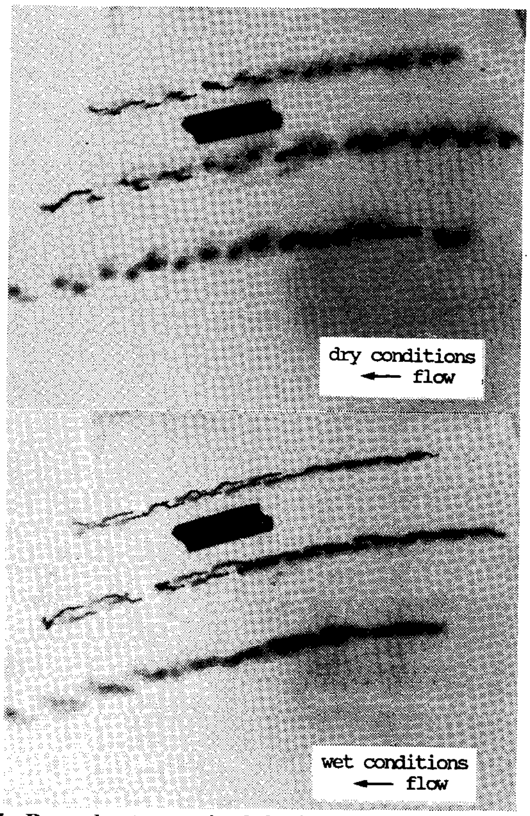

Fig. 15 Dry and wet separation behavior of the NACA 64-210 airfoil at 12-deg angle of attack.

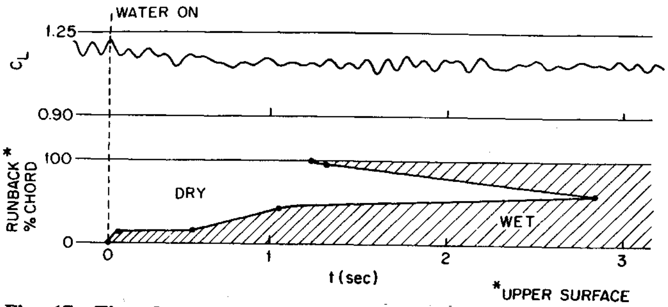

Fig. 17 Time-dependent lift and water runback position for the Wortmann FX67-K170 airfoil at 15-deg angle of attack.

equivalent. However, the NACA 0012 losses occur in the first 0.15 s, while the NACA 64-210 losses occur over a longer time scale of about 2 s. Both the liquid crystal observations and the CFD code indicate that boundary-layer transition occurs at about 75% chord for the NACA 64-210 airfoil at 1-deg angle of attack in dry conditions. When transition is forced at the leading edge in the CFD code, the performance degradation is again consistent in magnitude with the experimental results. There is one additional observation for the NACA 64-210 airfoil. Less water is present on the NACA 64-210 airfoil surface compared to the other two airfoils. This is due to the relative thinness of the airfoil and the high curvature of the leading edge. A direct result of the lower water quantities on the NACA 64-210 airfoil is the unexpected high water runback velocities after 50% chord (Fig. 13) created when the water rivulets break up into individual drops that run back at higher velocities.

High-Angle-of-Attack Behavior

The steady-state output of the airfoils at high angles of attack appears significantly different from the low-angle-of-attack behavior (Figs. 4–6). The methods used to analyze the heavy rain effects at high angles of attack are similar to those discussed previously. However, due to convergence problems resulting from the strongly separated regions at high angles of attack, the CFD code could not be used in this regime. Because the NACA 64-210 airfoil showed the most unexpected high-angle-of-attack behavior in rain conditions (Fig. 6), it was studied in greatest detail at high angles of attack, and its results will be presented first.

NACA 64-210 Airfoil

At high angles of attack, the NACA 64-210 airfoil exhibits unexpected increases in lift and decreases in drag in wet conditions (Fig. 6). Time-dependent lift output is shown in Fig. 14 for the NACA 64-210 airfoil at 15 deg angle of attack. The lift increase occurs within 0.3 s after entering the rain conditions. The water layer is present only in the first 10% of the chord, which indicates a leading-edge phenomenon is causing the performance enhancement. In fact, top surface water runback on the airfoil did not begin until about 2 s after the rain was initiated (Fig. 14).

Separation behavior as observed with microtufts is shown in Fig. 15 for the NACA 64-210 airfoil in dry and wet conditions at 12-deg angle of attack. The photograph of the dry condition indicates that a severe leading-edge separation is present. The photograph in the wet condition, however, indicates that the leading-edge separation is not present and that the flow is attached to at least the 50% chord position. As at low angles of attack, the rain is believed to cause premature boundary-layer transition. This is thought to increase the mixing and energize the boundary layer, making it less susceptible to separation.

Similar performance increases and flow reattachment have been observed at high angles of attack for airfoils subjected to extreme sound levels.[12] The mechanism is thought to be similar to the premature boundary-layer transition caused by rain, but is not well understood.

NACA 0012 Airfoil

The NACA 0012 airfoil exhibits similar high-angle-of-attack behavior to the NACA 64-210 airfoil. The NACA 0012 airfoil in dry conditions has a rather drastic stall at 14-deg angle of attack (Fig. 5). However, in rain conditions stall is delayed to 18 deg. This effect is a direct result of the premature boundary-layer transition induced by the rain, which suppresses stall. Figure 16 shows the rapid lift increase for the NACA 0012 airfoil at 15-deg angle of attack when rain is initiated. There is also a slow, secondary lift loss, which corresponds to the time scale of the water runback. Downstream of 60% chord, the water runback becomes nearly stagnant, indicating a trailing-edge separation at that point. The trailing-edge separation in wet conditions does not degrade the airfoil performance as much as the leading-edge separation, which occurs in dry conditions.

Wortmann FX67-K170 Airfoil

At high angles of attack in dry conditions, the aerodynamic behavior of the Wortmann airfoil is very complicated (Fig. 4). This may be due to the coupling of various separation mechanisms, such as laminar separation bubbles and trailing-edge separation.[13] In contrast, the high-angle-of-attack behavior in wet conditions (Fig. 4) is typical of an airfoil with a turbulent boundary layer. The stall is gradual as the trailing-edge boundary-layer separation point moves forward with increasing angle of attack. Figure 17 shows the lift output as a function of time at 15-deg angle of attack when rain is initiated. It is interesting to note that the lift degradation occurs slowly when compared to low-angle-of-attack behavior.

Summary and Conclusions

Wind-tunnel experiments at a Reynolds number of 3.1×10^5 and a rain rate of 1000 mm/h have been conducted in dry and wet conditions to compare the quantitative and qualitative aerodynamic performance degradation of a Wortmann FX67-K170, an NACA 0012, and an NACA 64-210 airfoil in heavy rain conditions. These tests were conducted to determine the mechanisms that affect airfoil performance in rain conditions at subscale and as a preliminary evaluation of potential heavy rain mechanisms induced at higher scales. In addition, these test results may help resolve the scaling problems associated with experimental heavy rain testing.

Two primary effects of rain were observed at significantly different time scales. The initial effect of rain is to cause premature boundary-layer transition near the leading edge immediately upon entering the rain condition. This effect caused performance degradation for all three airfoils at angles of attack below stall initiation. Lift was decreased by as much as 25% for the Wortmann airfoil. At high angles of attack, the premature boundary-layer, transition reduced separated flow regions and suppressed stall for the NACA 64-210 and 0012 airfoils. For the Wortmann airfoil at high angles of attack, lift was still reduced in wet conditions, but the lift curve was smoothed.

The other primary effect of rain occurred over longer time scales consistent with the water runback behavior. The water layer is believed to alter the airfoil geometry. The absolute magnitude of the performance losses due to these geometric effects was small and nearly equivalent for all three airfoils. It should be noted, however, that because of the small scale of the models employed in these experiments, the ratio of the water layer thickness to the chord length is artificially high. Therefore, the significance of the water layer shape changing effects is likely enhanced in these small-scale tests.

The magnitude of the rain effect varied greatly between the airfoils and appeared to be related to the susceptibility of each airfoil to premature boundary-layer transition. The Wortmann airfoil, which is a naturally laminar flow airfoil, had significant performance degradation in heavy rain conditions due to the premature boundary-layer transition mechamism. The NACA 0012 airfoil had some losses in heavy rain, and the NACA 64-210 airfoil had minimal degradation. However, each airfoil at low angles of attack had a significant laminar boundary-layer region. The susceptibility of the airfoils to heavy rain at low angles of attack could be emulated by forcing boundary-layer transition near the leading edge.

The low Reynolds number test results appear to be important when considering low Reynolds number vehicles such as mini-RPVs and sailplanes. In addition, because high-lift multielement airfoils are carefully designed to optimize the interaction of the boundary layers between components,[14] the overall aerodynamic performance of the multielement airfoil may be deoptimized in rain conditions as a result of the boundary-layer effects on individual elements. It is recognized that because of the low Reynolds number test condition, the results of these tests may not be directly extrapolated to higher Reynolds number cases. However, the physical mechanisms of the water behavior and their importance may be similar at larger scales.

Acknowledgments

This work was supported by the National Aeronautics and Space Administration under Grant NAG-1-568.

References

[1]Haines, P. and Luers, J., "Aerodynamic Penalties of Heavy Rain on Landing Airplanes," *Journal of Aircraft*, Vol. 20, Feb. 1983, pp. 111–119.

[2]Yip, L. P., "Wind-Tunnel Investigation of a Full-Scale Canard-Configuration General Aviation Airplane," NASA TP-2382, March 1985.

[3]Dunham, R. E., Bezos, G. M., Gentry, C. L., and Melson, E., "Two-Dimensional Wind Tunnel Tests of a Transport-Type Airfoil in a Water Spray," AIAA Paper 85-0258, Jan. 1985.

[4]Dunham, R. E., "Potential Influences of Heavy Rain on General Aviation Airplane Performance," AIAA Paper 86-2606, Sept. 1986.

[5]Hansman, R. J. and Barsotti, M. F., "The Aerodynamic Effect of Surface Wetting Characteristics on a Laminar Flow Airfoil in Simulated Heavy Rain," AIAA Paper 85-0260, Jan. 1985.

[6]Marchman III, J. F., Robertson, E. A., and Emsley, H. T., "Rain Effects at Low Reynolds Number," AIAA Paper 87-0258, Jan. 1987.

[7]Rhode, R. V., "Some Effects of Rainfall on Flight of Airplanes and on Instrument Indications," NACA TN 803, April 1941.

[8]Holmes, B. J., Croom, C. C., Gall, P. D., Manuel G. S., and Carraway, D. L., "Advanced Boundary Layer Transition Measurement Methods for Flight Applications," AIAA Paper 86-9786, 1986.

[9]Drela, M., "Two-Dimensional Transonic Aerodynamic Design and Analysis Using the Euler Equations," Ph.D. Thesis, Department of Aeronautics and Astronautics, Massachusetts Institute of Technology, Cambridge, MA, 1985.

[10]Giles, M. B., "Newton Solution of Steady Two-Dimensional Transonic Flow," Ph.D. Thesis, Department of Aeronautics and Astronautics, Massachusetts Institute of Technology, Cambridge, MA, 1985.

[11]Bisplinghoff, R. L. and Ashley, H., *Principles of Aeroelasticity*, Dover, 1962, pp. 114–125.

[12]Collins, F. G. and Zelenevitz, J., "Influence of Sound Upon Separated Flow Over Wings," *AIAA Journal*, Vol. 13, March 1975, pp. 408–410.

[13]Muller, T. J., "Low Reynolds Number Vehicles," AGARD AG-288, 1985.

[14]Smith, A.M.O., "High Lift Aerodynamics," *Journal of Aircraft*, Vol. 12, June 1975, pp. 501–503.